

# 1. Background and Introduction

FEMA FLOOD INSURANCE RATE MAP (FIRM) guidelines do not currently exist for conducting and incorporating tsunami hazard assessments that reflect the substantial advances in tsunami research achieved in the last two decades. Thus, current FIRMs rely heavily on the science, technology, and methodologies developed in the 1970s, such as that of Houston and Garcia (1974) and Houston (1980). This work is generally regarded as groundbreaking and state-of-the-art for its time, but is now superseded by modern methods (Table 1).

Two recent FEMA workshops were held to help develop plans for updating the existing FIRMs. The approximately 40 workshop participants included FEMA management, coastal engineering and scientific experts, floodplain management professionals, and study contractors. FEMA guidance at the first workshop encouraged a regional approach, in recognition that “one shoe seldom fits all” and that somewhat different methodologies are frequently required to properly account for regional differences. The second workshop concentrated on reviewing “Focused Study” plans developed by Technical Working Groups, including the Tsunami Focused Study.

**Table 1:** Comparison of pre-1990 and post-1990 tsunami hazard assessment.

Component	Pre-1990	Post-1990
<b>Runup modeling</b>	No	Yes
<b>Far-field sources</b>	Earthquakes. Surface deformation based on simple elliptic analytic idealizations.	Earthquakes and landslides. Surface deformation based on geophysical models.
<b>Near-field sources</b>	No. Importance not recognized.	Yes. Importance now recognized as a result of numerous studies.
<b>Bathymetry and topography</b>	Low quality coverage and availability. Deep ocean modeled as constant-depth basin. Shallow coastal features not adequately resolved.	Improved quality, coverage, and availability of Pacific deep and coastal bathymetry and topography.
<b>Computational grids</b>	Coarse-resolution.	Fine-resolution, where required.
<b>Probabilistic methodology</b>	Based on short-term historical tsunami record.	Based on long-term paleoseismic and paleotsunami records and short-term, historical earthquake and tsunami records.
<b>Hazard zone identification</b>	Qualitative estimates inferred from offshore height only.	Indices can be computed, based on both runup heights and currents.

Tsunamis generated by seismic or other sources near or far from a site of interest are termed, from the point of view of that site, *near-field* (or *local*) and *far-field* (or *distant*) tsunamis, respectively. The Tsunami Focused Study (Tsunami Focused Study Team, 2005) identified two general types of sources as the most common generators of destructive tsunamis: earthquakes, which might be local or distant from the area of interest; and slides, which might be coseismic or aseismic, subaerial or subaqueous.

Earthquake sources generally produce a zone of destructive tsunami energy over a larger geographic scale than slide sources. Differences in the relative importance of local and distant earthquake sources serve to identify five distinct Pacific Tsunami Regimes:

- A. *Southern and Central California*. Local offshore fault systems; distant Subduction Zones
- B. *Cascadia (Northern California to Northern Washington and Straits of Juan de Fuca)*. Local Cascadia Subduction Zone; distant subduction zones
- C. *Puget Sound*. Local Seattle, Tacoma, and other fault systems
- D. *Alaska*. Local Alaska-Aleutian Subduction Zone
- E. *Hawaii*. Distant subduction zones

Slide sources in all regions can also generate tsunamis that produce destructive zones, but on a smaller geographical scale, with variations in the type and potential threat. Upon review and discussion by workshop participants of the Tsunami Focused Study plan, the following recommendation was made:

“The recommended approach is to perform a comprehensive probabilistic tsunami hazard assessment at a pilot site in California or Oregon or Washington [that includes]: (1) recurrence interval estimate[s] of forcing functions and (2) propagation of tsunamis from Pacific Seismic subduction zones, (3) inundation calculations, [and] (4) probability distributions and integration.”

Subsequently, after a site selection study, this interagency project—the Seaside Tsunami Pilot Study—was funded by the FEMA Map Modernization Program. The purpose of the study was to develop methods and preliminary guidelines for future tsunami components of FEMA FIRMs. These specific guidelines would apply to coastal communities along the coast of the Cascadia Tsunami Regime, extending from Cape Mendocino to the Strait of Juan de Fuca. Existing FEMA Flood Insurance Studies and the resulting FIRM maps for this region do not include tsunamis as a flooding hazard. During the 1970s, a Type 16 Flood Insurance Study was carried out for this region by Houston and Garcia (1978). Their study was based on the assumption that only far-field tsunamis impacted this region. Furthermore, their computations did not include actual inundation of the land. Since that study, compelling evidence from earthquake and paleotsunami research has shown that great earthquakes occur in the Cascadia Subduction Zone and that these earthquakes generate

major tsunamis. These local Cascadia events, although infrequent, are not rare. Furthermore, they would cause such widespread and severe devastation that they need to be considered in developing new FIRM maps for this coastal region.

The site for the Pilot Study includes the communities of Seaside and Gearhart, Oregon, and the adjacent unincorporated areas. The site was chosen because it is typical of coastal communities in the region with development on sand spits and other low-lying areas near the ocean and with coastal rivers flowing through the communities. The study area was also recommended by Oregon Emergency Managers, who need the results of the Study for tsunami evacuation planning and public education. Furthermore, stakeholders in the Seaside/Gearhart area are very interested in tsunamis, due in part to the flooding and damage caused by the 1964 Alaska tsunami and other recent tsunamis that struck these communities. There is also increased awareness that major Cascadia Subduction Zone tsunamis have struck this area in the past.

This pilot study directly addresses Task Item 16, “Probabilistic Hazard Assessment for the open and non-open coastlines of the Pacific States,” and Task Item 20, “Tsunami structure debris interaction to define hazard zones,” identified in a series of workshops in 2004 that were held to plan the development of new tsunami hazard mapping guidelines for FEMA’s National Flood Insurance Program. A methodology was recommended for a comprehensive probabilistic tsunami hazard assessment for the Cascadia Region, considering both far-field events and near-field events triggered by seismic sources. For both types of events, the tsunamis are generated by coseismic seafloor displacement and submarine landslides. Far-field events are defined as those generated a long distance away by sea floor displacement during earthquakes, such as the 1964 Alaska and 1960 Chile earthquakes; near-field events are those generated by sea floor displacement from Cascadia Subduction Zone earthquakes. An example of the latter is the 1992 Cape Mendocino tsunami that was incident on the northern California coast (González *et al.*, 1995).

FEMA’s policy has been to incorporate tsunami-induced hazards and other storm-related coastal hazards into one coastal high-hazard zone, which is defined in the Code of Federal Regulations, Title 44, Part 59.1 as:

Coastal high hazard area means an area of special flood hazard extending from offshore to the inland limit of a primary frontal dune along an open coast and any other area subject to high velocity wave action from storms or seismic sources.

During the course of the present study, it became imperative to address not only the statistical aspects of tsunami generation but also the associated geological, numerical modeling, regulatory, and institutional aspects as well as the available resources in NOAA, USGS, and academic institutions participating in this study.



## 2. Previous Methods Used for FIRM Tsunami Maps

FOR THE FEMA PILOT STUDY, it is helpful to understand the procedures used by Houston and Garcia (1978) to develop the previous set of FIRM tsunami maps for the U.S. West Coast. Like the goals of the new Pilot Study, their procedures produced 100- and 500-year tsunami runup elevations using numerical models and probabilistic approaches to both the distribution of tsunami sources, in terms of their intensity and location, and the effects of tides and other background water levels on the elevations. The purpose of this section is to summarize the assumptions and methodology used by Houston and Garcia (1978) in order to provide background for the Pilot Study and to provide a perspective when comparing their results with those generated by the Pilot Study. Only a few references are given in this section; an extensive bibliography can be found in the 1978 report.

When Houston and Garcia (1978) did their study for the Federal Insurance Administration in the Department of Housing and Urban Development, regional tsunami sources in the Cascadia Subduction Zone had not been identified as the most likely to dominate the 100- and 500-year tsunami runup elevations along the middle and northern portions of the West Coast. Local landslides in the Southern California Bight had also not been identified as important sources for that region. However, Houston and Garcia (1978) state that important local sources might eventually be found but that such sources are outside the scope of their study. The sources they use are limited to the Alaska-Aleutian and Peru-Chile Subduction Zones, justified by the historical record of damaging tsunamis along the West Coast.

### 2.1 Tsunami Sources

The tsunamis striking the West Coast are assumed by Houston and Garcia (1978) to be teletsunamis from the Alaska-Aleutian and Peru-Chile Subduction Zones. Using observed tsunamis in the source regions, the tsunami intensities  $i = \log_2(2^{1/2}R_{\text{avg}})$  are first computed from the average runup height  $R_{\text{avg}}$  in meters using the Imamura-Iida intensity scale as modified by Soloviev (1970). (Runup is strictly defined as the wave height at maximum inundation. As used in this case, runup is a more general term that also describes wave height measurements within the inundation zone.) A least-square fit to the historical data along the Peru-Chile Subduction Zone then gives  $n(i) = 0.074e^{-0.63i}$  as the probability of occurrence in a given year for a tsunami of intensity  $i$ . (The Houston and Garcia (1978) technical report lacks the minus sign

in the exponential term, which is needed since the probability  $n(i)$  should decrease with increasing tsunami intensity.) Since there is much less historical information on tsunamis occurring in the Alaska-Aleutian Subduction Zone, an assumed exponent coefficient  $-0.71$  is used, i.e.,  $n(i) = 0.113e^{-0.71i}$ , based on large ( $i =$  or  $> 3.5$ ) tsunamis in the Alaska-Aleutian Subduction Zone and observed coefficients of other tsunamigenic regions around the Pacific (Soloviev, 1970). The probabilities are assumed to be uniform along the respective subduction zones.

The Alaska-Aleutian Subduction Zone is divided into 12 segments and the Peru-Chile Subduction Zone into 3 segments. The fine segmentation along the Alaska-Aleutian Subduction Zone honors the observation that the heights of tsunamis along the West Coast are very sensitive to the location of earthquake in the Alaska-Aleutian Subduction Zone, whereas this is much less true for the Peru-Chile Subduction Zone. The coseismic uplift patterns due to the tsunamigenic earthquakes are assumed to be ellipses oriented parallel to the subduction zone trench and are centered on the respective segment.

The shapes and sizes of the uplift ellipses are “standardized” because there is often a disparity between the intensity, observed uplift extent, and the tsunami heights that occur at impact site. Houston and Garcia (1978) discuss this issue using the 1946 and 1957 Aleutian tsunamis, in which the modest 1946 earthquake had a relatively small uplift area but large tsunami, whereas the great 1957 earthquake had a very large extent but a much smaller teletsunami. Other issues and their implication for tsunami generation are also discussed.

For each segment, seven tsunami intensities in the range  $i = 2 - 5$  (in increments of 0.5) are used. Here,  $i = 2$  is considered a lower limit for dangerous tsunamis along the West Coast; and  $i = 5$  is a credible upper limit based on the history of Pacific tsunamis. The 15 earthquake segments (12 for the Alaska-Aleutian and 3 for the Peru-Chile Subduction Zones) then lead to a total of 105 tsunami sources used in the study by Houston and Garcia (1978), each with its own probability of occurrence.

## 2.2 Trans-Pacific and Nearshore Numerical Models

A linear finite difference model ( $1/3^\circ \times 1/3^\circ$ ) is used to propagate the tsunamis from each source across the Pacific to the vicinity (about the depth contour of 500 m) of the West Coast. The details of the trans-Pacific model are given in Houston and Garcia (1974). A finer-scale nearshore finite difference model ( $2' \times 2'$ ), driven by tsunami time series at the open boundaries, is then used to estimate runup along a vertical-wall coast. The nearshore model is based on that of Leendertse (1967) and includes advective terms and quadratic drag.

The West Coast is divided into four overlapping segments, each with its own nearshore model applied to a rectangular domain. Variable bathymetry is used out to the 500 m depth contour, beyond which the depth is set to 500 m. Each domain has a normal-to-shore width of approximately 1.5 wavelengths of a 30-min tsunami. This width is chosen so that at least three waves of a major trans-

Pacific tsunami have a chance to reach the coast before re-reflection can occur at the open seaward boundary.

While the southern domain extends across half of the Southern California Bight, only results for the region west of Santa Barbara are reported. However, 100- and 500-year tsunami maps for the Southern California Bight are given by Houston and Garcia (1974). Likewise, Garcia and Houston (1975) show analogous maps for Monterey and San Francisco Bays and Puget Sound.

Verification of the model time series is limited to a comparison at Crescent City and Avila Beach (Port San Luis), California. There is significant disagreement at Crescent City, but this station had only a partial tide gage record. The agreement at Avila Beach (largest tsunami amplitude reported from uninterrupted 1964 tide gage records along the West Coast) is good and is taken to be justification for the modeling procedures.

## 2.3 Predicted Tides

To include the effects of the tides on the maximum tsunami runup elevation, Houston and Garcia (1978) use as tidal input 15-min sampled time series of predicted tides for stations along the West Coast. Observed NOAA harmonic constants were used to compute the predicted tides where these were available. Presumably the predicted tides were either zoned (constant within a coastal section) or interpolated to give the coastal tides at the nearshore model grid points. The tidal time series are for the year 1964, during which nodal factors modifying tidal heights are at or near their average values during the 18.6-year nodal cycle. Clearly, these are also convenient series to use when discussing the 1964 Alaska tsunami.

## 2.4 Computing the 100- and 500-Year Tsunami Runup Heights

For each of the 105 tsunami time series at each coastal grid point of the nearshore model, a 24-hr tsunami series is prepared by adding a sinusoidal series (with an amplitude equal to 40% of the maximum height of the first model waves) to the 2 hr of directly modeled series representing the first waves of the tsunami. The factor of 0.4 was determined from observed tsunamis along the West Coast that are observed to decay slowly in time. Adding a given tsunami time series sequentially to the predicted tide, stepping every 15 min, and then computing the maximum height of the combined tsunami and tide, leads to a year-long series of maximum runup heights. The largest of these is selected to give the tsunami runup elevation for that coastal grid point and that tsunami source location and intensity. This is under the assumption that the linear sum of the tsunami and tidal time series adequately represents the actual water levels for that tsunami impacting the coast as the tides vary in time.

The 100- and 500-year tsunami runup heights are computed numerically by Houston and Garcia (1978) from the maximum runup heights and probabilities

**Table 2:** 100- and 500-yr tsunami runup heights at Seaside, Oregon (latitude of 46° 00.0'N) relative to various tidal datums. The heights are computed from the Houston and Garcia (1978) results relative to mean sea level (MSL), using observed tidal datums interpolated in latitude between Hammond (46° 12.1'N, 123° 56.7'W) and Garibaldi (45° 33.3'N, 123° 45.7'W).

	Datum (m)*	100-Year Runup (m)	500-Year Runup (m)
MHHW	2.5	2.1	4.7
MHW	2.3	2.3	4.9
MTL	1.4	3.2	5.9
MSL	1.3	3.2	5.9
MLW	0.4	4.2	6.9
MLLW	0.0	4.6	7.3

\*1983–2001 Tidal Epoch

associated with the corresponding source segment and tsunami intensity. For a given coastal grid location, the probabilities are summed over decreasing heights starting with the maximum one for that location. When the sum reaches 1/500, this is the 500-year runup height for that coastal location. The summing of the individual probabilities downward in height then continues until the summed probability reaches 1/100, yielding the 100-year runup height. Once this is done for all the coastal grid points along the West Coast, smooth curves are drawn through these to give the alongshore distributions of the 100- and 500-year runup heights that are shown in Plates 1–30 of Houston and Garcia (1978).

## 2.5 Application to Seaside, Oregon

Shown in Table 2 are the 100- and 500-year tsunami runup heights computed from Plate 26 of Houston and Garcia (1978) for Seaside, Oregon, which is the site location for the FEMA FIRM Pilot Study. The heights are for the open coast at lat. 46° 00.0'N, which passes through Seaside. The original heights are in feet relative to mean sea level (MSL). For the purposes of the Pilot Study and for other applications, Table 2 also contains heights relative to other tidal datums on the open coast.

Mean high water (MHW) was used as the background water level for all inundation modeling performed in the current study. A check on the consequences of fixing the background water level at MHW was made by performing a statistical analysis based on linearly superimposed tsunami wavetrains by predicted tides at Seaside. The tsunami wavetrains are assumed to decay exponentially in time with an e-folding decay coefficient of 2.0 days, consistent with observed Pacific teletsunamis (Van Dorn, 1984; Mofjeld *et al.*, 2000). Assuming a linear superposition may be regarded as a first step toward a fuller analysis that includes the dynamical interaction between tsunamis and the tides. The details of the linear analysis are given by Mofjeld *et al.* (in press). It is consistent with the way the Seaside tides are included in the estimation of the 0.01- and 0.002-probability wave heights in this present study (see Appendix E).

**Table 3:** Representative maximum tsunami wave heights when the background water level in the tsunami inundation model was set to mean high water (MHW) and when the equivalent mean height for the tsunami wavetrain was superimposed linearly on predicted Seaside tides (1992).

<b>Annual Prob.</b>	<b>Location</b>	<b>Background: MHW (m)</b>	<b>Adjusting for Tides (m)</b>	<b>Difference (m)</b>	<b>Difference (%)</b>
0.01	Coastal	4.0	3.6	0.4	10
	Estuarine	3.0	2.8	0.2	8
0.002	Coastal	10.0	9.3	0.7	8
	Estuarine	7.0	6.5	0.5	7

Briefly summarizing the results of the Mofjeld *et al.* (in press) analysis, the probability distribution functions (pdfs) of maximum wave height for small tsunamis (<0.5 m amplitudes) are tightly concentrated around the sum of the tsunami amplitude and mean higher high water (MHHW). Hence, using MHW as the background water level in modeling these small-amplitude tsunamis introduces a slight downward bias relative to the mean height of the pdfs. At Seaside, this bias amounts to MHHW–MHW = 0.23 m. As the amplitude of the incident tsunami increases, the pdf changes both in mean maximum height and vertical spread. The total mean is the sum of the tsunami amplitude at each location and an effective height. The latter decreases from MHHW to mean sea level (MSL) with increasing amplitude. For very large tsunami amplitudes, the largest tsunami wave simply selects the stage of the tide at the time of the wave crest. Statistically, the pdf then represents the probability distribution of the tide itself.

For the 0.01- and 0.002-probability wave heights shown in Figs. 26 and 28, the effect of not allowing the tides to vary in the tsunami modeling gives an upward bias (Table 3) of 0.2–0.7 m (7–10%) based on the linear analysis. The bias will be less at other locations where the tsunami amplitude is less, so the values in Table 3 are estimates of the maximum bias.

There is a need for future research on non-linear tide/tsunami interactions and their effects on wave heights, inundation, and current strength. Research is also needed on issues of tsunami-caused erosion during the first waves that might alter the access of tsunamis and tides to estuaries and coastal rivers.



### 3. Development of GIS Database

**A**N EXTENSIVE AMOUNT of relational spatial data was collected and developed for the study. A geographic information system (GIS) was built to organize these data for analysis (Wong *et al.*, 2006). The GIS database consists of data descriptions, preview images, virtual globe (Google Earth©) views, metadata, and downloadable files (Table 4). Except for data sets strongly tied to the study, such as historic inundation lines and existing FEMA Flood Insurance Rate maps, the GIS serves only data developed in the course of building the tsunami model.

The majority of the data were built using ESRI ArcGIS© software products. All were georeferenced to the following parameters:

- Coordinate system: Geographic decimal degrees or Universal Transverse Mercator Zone 10 where indicated
- Vertical units: Meters
- Horizontal datum: North American Datum of 1983
- Vertical datum: Mean High Water

**Table 4:** Summary of GIS database layers.

Category	Dataset
Digital elevation model development	Coastal tide stations Modeling grid limits Historic shorelines Vertical control data Seaside digital elevation model
Historical tsunami events	Alaska 1964 event deposits, observations, and inundation Cascadia 1700 event deposits and inundation Photographs of field sites
Tsunami propagation and inundation modeling	Far- and near-field earthquake sources Maximum tsunami velocity zones based on far- and near-field sources Coseismic vertical displacement fields for near-field sources Maximum wave heights based on far- and near-field sources
Probabilistic tsunami hazard assessment model	Probability surfaces for maximum wave heights of 0.5 to 10.5 m Maximum tsunami wave heights for 100- and 500-year floods

The horizontal datum was based on the latest accepted geodetic references. Mean High Water (MHW) was used as the constant background water level for the tsunami inundation modeling, and this is the reference datum for the tsunami heights in this report. Current FEMA FIRM maps are based on the horizontal and vertical datums of the North American Datum of 1927 and the National Geodetic Vertical Datum of 1929, respectively. Mofjeld *et al.* (2004) provide more information on the determination of vertical datum values for Seaside (Appendix A).

### 3.1 Digital Elevation Model

An accurate digital elevation model (DEM) is critical to accurate model results. The DEM for inundation modeling should consist of the best available elevation data at a resolution of 50 m or less (González *et al.*, 2005). Elevation data available from Federal, State, and local agencies often consist of disparate horizontal and vertical datums that must be rectified through accepted conversion methods (see Appendix A).

Three nested DEMs were created for the MOST model to simulate tsunami generation at the offshore source, wave propagation nearshore, and inundation in the region of interest (Fig. 1, Table 5). The source and propagation DEMs consist solely of bathymetric values with land set to a “no data” value. The inundation DEM consists of both bathymetric and topographic values.

These DEMs were developed using a standard four-step process:

1. Data collection
2. Data assessment
3. DEM development
4. Quality assessment

The best available bathymetric, topographic, orthophotographic, and control data were obtained from various government agencies and converted to modeler parameters. Datasets were analyzed for accuracy and consistency. The best available data were used to build the DEMs.

The inundation DEM was compared to fifteen vertical control points to yield a RMS error of 0.135 m. Detailed procedures, methodologies, and quality assurance analyses are available in Venturato (2005) (Appendix B).

Significant shoreline differences were discovered when comparing the inundation DEM with historical shorelines. Coastlines extracted from regional

**Table 5:** DEM summary.

Region	Resolution	SW/NE Corner Extents
Pacific Northwest (bathymetry only)	36 arc-seconds (~1 km)	SW: -132.00, 43.00; NE: -122.00, 53.00
Washington-Oregon Border (bathymetry only)	6 arc-seconds (~180 m)	SW: -124.5, 45.36; NE: -123.5, 47.36
Seaside	1/3 arc-seconds (~10 m)	SW: -124.04, 45.90; NE: -123.89, 46.08

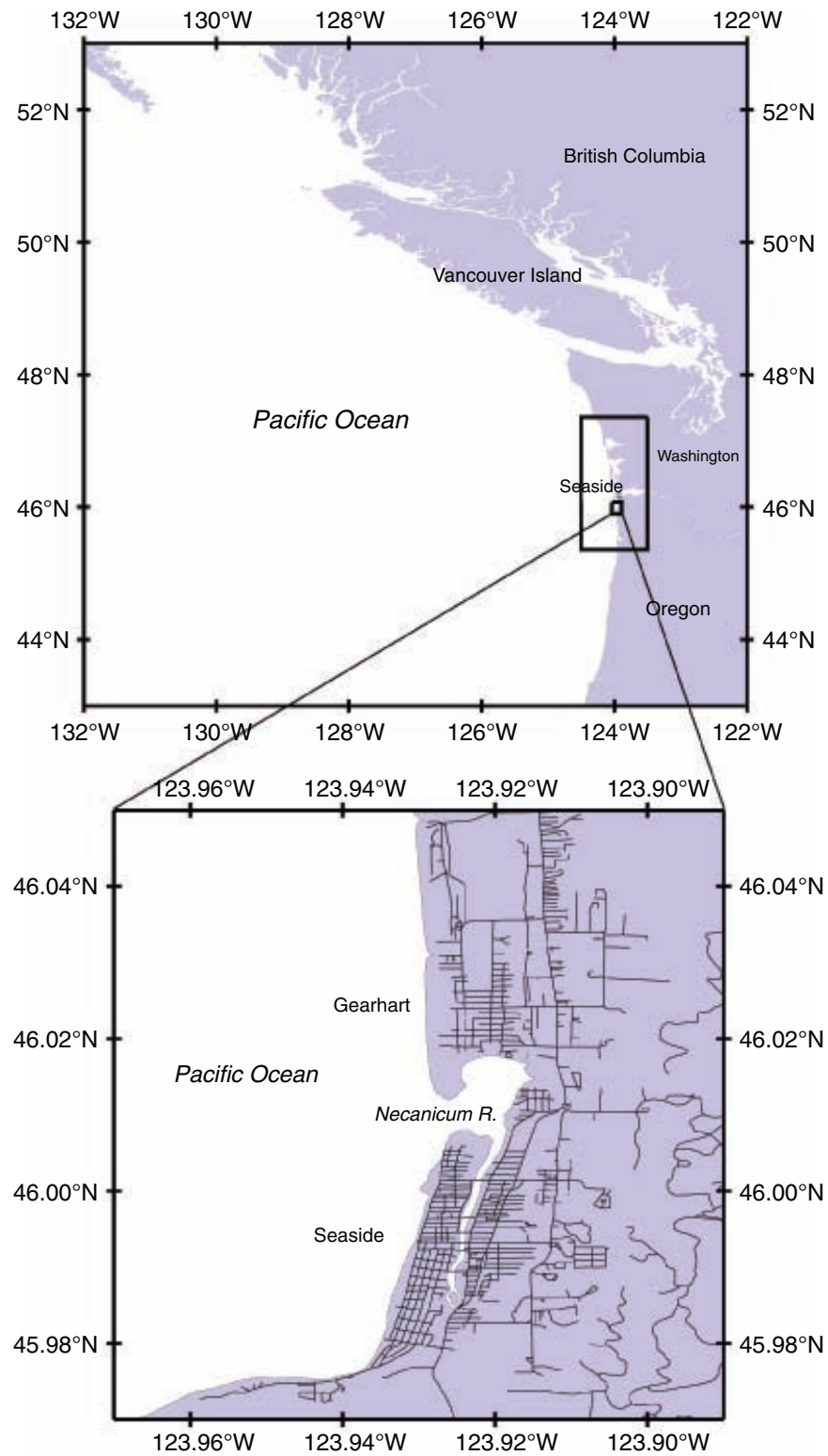


**Figure 1:** Study area of the FEMA FIRM pilot project for Seaside, Oregon. Top panel displays nested grids used by the model. Bottom panel details the study region.

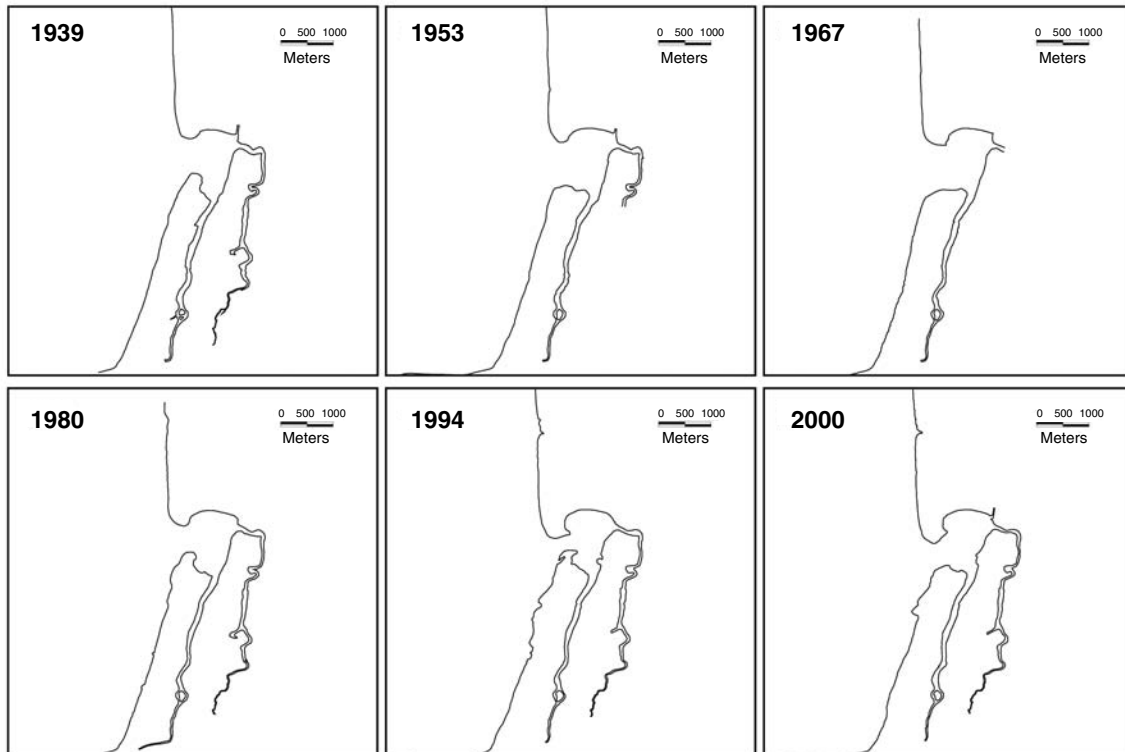


**Figure 2:** Historical shoreline depicting the apparent Mean High Water line based on orthophotography from various Federal and State agencies.

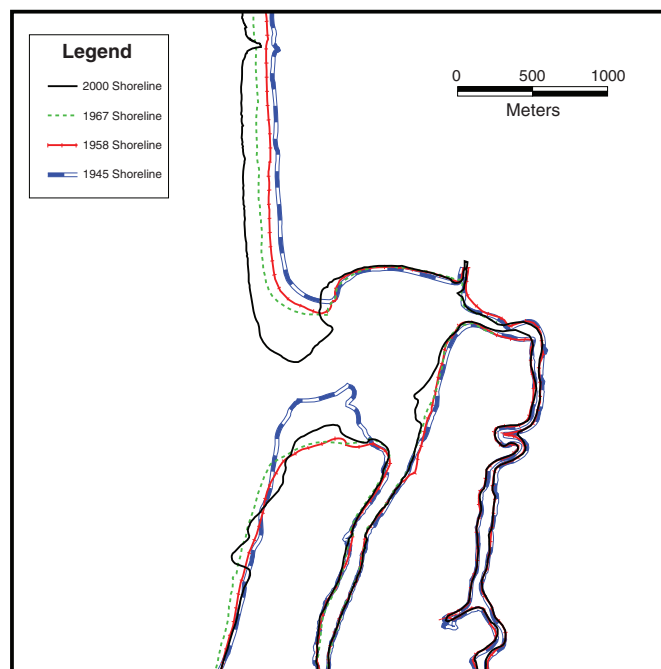


**Figure 3:** Accretion and erosion trends of the Necanicum River mouth (3.2 m/y).

historical aerial photography obtained from the University of Oregon show a general trend of accretion averaging 3.2 m/yr on the outer coast north of the Necanicum River mouth (Fig. 2) (Appendix B).

A cyclic pattern of erosion and accretion within the Necanicum River mouth along its northern and southern Mean High Water extents is apparent (Fig. 3). The northern extent generally shows an accretion rate of approximately 7 m/yr since 1939. The southern extent varies between accretion and erosion over an estimated 15-year cycle. The river mouth cycled from a minimum width of 300 m to a maximum width of 800 m over the 65-year period (Appendix B).

The final DEMs were distributed in an ASCII raster format to the modeler. The modeler converted the DEMs to a format compatible with the model, clipped the DEM to cover the inundation area, and applied an algorithm to smooth the bathymetry using a predetermined steepness threshold (refer to the Section 6, “Propagation and Inundation Modeling”).

## 3.2 Historical Tsunami Event Data

Tsunami deposits, observations, and inundation lines were collected to compare with model results. Deposits collected in the field (see Tsunami Deposits section) were converted to GIS files for comparison with model results. Estimated inundation lines were subsequently created for the 1964 Gulf of Alaska and the 1700 Cascadia Subduction Zone events. Summaries of observations and historic shoreline are discussed below.

### 3.2.1 Observations

Over 70 observations at Seaside of the 1964 Gulf of Alaska event were added to the GIS database for comparison (Fiedorowicz, 1997) (see also Appendix C). These observations include estimated runup/wave height values and type (Fig. 4).

### 3.2.2 Shoreline

The apparent Mean Lower Low Water line was digitized (Fig. 5) from orthophotos nearest in time to significant historical tsunami events (1946 East Aleutian Islands, AK, 7.3  $M_s$ ; 1960 Central Chile, 8.5  $M_s$ ; and 1964 Gulf of Alaska, 8.5  $M_s$ ). The Necanicum River mouth migrates northward from 1946 to 1964 and then southward from 1964 to 2000. The dynamic nature of the shoreline in this region could vary tsunami inundation patterns over time.

## 3.3 Model Output

Model runs from the Model Database (see Section 6, “Propagation and Inundation Modeling”) were converted to GIS-compatible formats and added to the GIS database. Model setup of the inundation grid introduced a rounding error

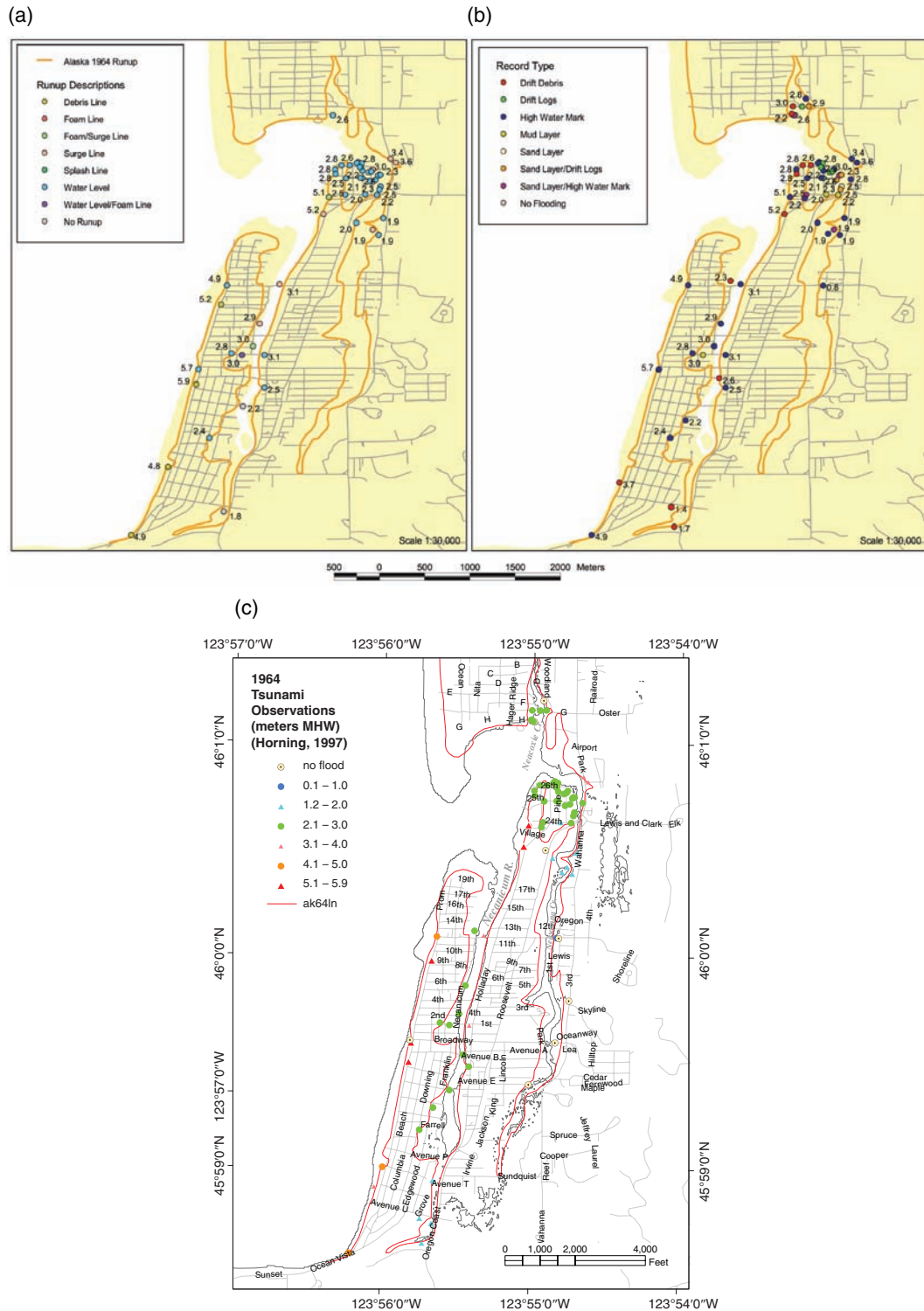


**Figure 4:** Observations of the Alaska 1964 tsunami event as described in Fiedorowicz (1997) and updated by Horning (see Appendix C). The runup line is based on observations (a) and tsunami deposits (b). The values associated with each observation represent runup elevation in meters based on a vertical datum of Mean High Water. Meaning of different eyewitness runup indicators listed in (a) described in Appendix C. Locations of possible tsunami sand and mud layers are provided in (b). (c) Major streets in Seaside and Gearhart shown with tsunami observation locations.

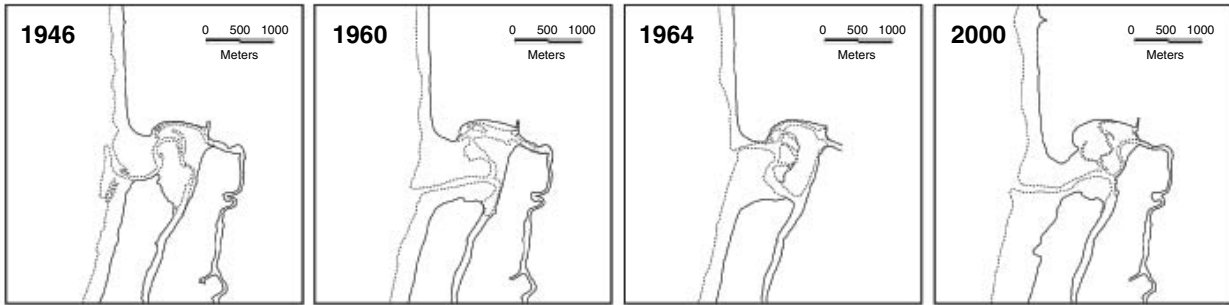


**Figure 5:** Estimated shoreline during historic tsunami events depicting Mean High Water (solid) and Mean Lower Low Water (dashed). Shoreline from the most recent orthophoto (2000) also displayed in rightmost panel.

(RMS error 0.000901 m), which is reflected in the model runs. Additional error (total RMS error 0.001267 m) was created during the conversion of the model runs to GIS. This error is considered insignificant in this study. Probabilistic tsunami wave height data were derived as described in the “Probabilistic Method” part of this report.